the accuracy of the method can be found from Hong et al. (1994a), Hong and Rubinsky (1994), and Hong (1993).

Conclusion

A new technique for analyzing problems of heat transfer with phase transformation in multiple domains was described. The technique employs interactive MRI imaging, thermocouple measurements, and finite difference analysis. The paper illustrates the ability of the technique to calculate the temperature distribution in multiple freezing domains that merge. MRI interactive heat transfer analysis may become an important tool in the armamentarium of researchers in heat transfer.

Acknowledgments

This research was supported by NIH grant No. RO1 CA56898-03A1.

References

Gilbert, J. C., Rubinsky, B., Roos, M. S., Wong, S. T. S., and Brennan, K. M., 1993, "MRI Monitored Cryosurgery in the Rabbit Brain," *Magnetic Resonance Imaging,* Vol. 11, pp. 1155–1164.

Hong, J. S., 1993, "Studies on the Use of Freezing for the Controlled Destruction and Preservation of Biological Tissue," PhD Thesis, University of California at Berkeley, Dept of Mechanical Engineering.

Hong, J. S., Wong, S., Pease, G., and Rubinsky, B., 1994, "MR Imaging Assisted Temperature Calculations During Cryosurgery," *Magnetic Resonance Imaging,* Vol. 12, No. 6, pp. 1021–1031.

Hong, J. S., and Rubinsky, B., 1994, "MR Imaging Assisted Temperature Calculations in Multiple Domain Freezing Problems," *Advances in Heat and Mass Transfer in Biological Systems,* L. J. Hayes and B. Roemer, eds., ASME HTD-Vol. 288, pp. 17–24.

Jaluria, Y., and Torrance, K. E., 1986, *Computational Heat Transfer,* Hemisphere Publishing Co., Washington DC.

Kaufman, L., Crooks, L. E., and Margulis, A. R., 1983, *Nuclear Magnetic Resonance Imaging in Medicine,* Igaku-Shoin Ltd., New York.

Keanini, R. G., and Rubinsky, B., 1992, "Optimization of Multiprobe Cryosurgery," ASME JOURNAL OF HEAT TRANSFER, Vol. 114, pp. 796–810.

Lunardini, V. J., 1981, *Heat Transfer in Cold Climates,* Litton Ed. Pub., Inc., New York.

Pease, G. R., Rubinsky, B., Wong, S. T. S., Roos, M. S., Gilbert, J. C., and Arav, A., 1994, "An Integrated Probe for Magnetic Resonance Imaging Monitored Skin Cryosurgery," ASME *Journal of Biomechanical Engineering,* in press.

Rubinsky, B., Gilbert, J. C., Onik, G. M., Roos, M. S., Wong, S. T. S., and Brennan, K. M., 1993, "Monitoring Cryosurgery in the Brain and in the Prostate With Proton MRI," *Cryobiology,* Vol. 30, pp. 191–199.

Boundary Layer Analysis of Buoyancy-Driven Two-Phase Flow in Capillary Porous Media

C. Y. Wang[1] and C. Beckermann[2]

Nomenclature

D = capillary diffusion coefficient = $(K/\nu)\lambda(1-\lambda)[-dp_c(s)/ds] \equiv D_c\hat{D}$

D_c = constant part of capillary diffusion coefficient = $(\epsilon K)^{1/2}\sigma/\nu_l$

$\hat{D}$ = dimensionless capillary diffusion function = $k_{rl}(1-\lambda)[-dJ(s)/ds]$

$f(s)$ = hindrance function = $k_{rv}\lambda$

F = dimensionless streamfunction, Eq. (15)

$\mathbf{g}$ = gravity vector

$\mathbf{j}$ = diffusive mass flux

$J(s)$ = capillary pressure function = $\mathbf{p}_c/[(\epsilon/K)^{1/2}\sigma]$

k = relative permeability

K = absolute permeability

p = mixture pressure = $p_v - \int_0^s \lambda(dp_c/ds)ds$

p_c = capillary pressure = $p_v - p_l$

q = heat flux

Ra = two-phase Rayleigh number = $Kg(\rho_l - \rho_v)x/(\nu_l D_c)$

s = liquid saturation

Sh = Sherwood number or dimensionless liquid mass flux at the wall = $j_w x/D_c$

$\mathbf{u}$ = Darcian mixture velocity vector = $\rho_l\mathbf{u}_l + \rho_v\mathbf{u}_v$

u = Darcian velocity in x direction

v = Darcian velocity in y direction

x = Cartesian coordinate

y = Cartesian coordinate

ϵ = porosity

η = similarity variable, Eq. (15)

λ = liquid relative mobility = $k_{rl}(s)/[k_{rl}(s) + \bar{\nu}k_{rv}(s)]$

μ = viscosity

ν = kinematic viscosity = $[k_{rl}(s)/\nu_l + k_{rv}(s)/\nu_v]^{-1}$

$\bar{\nu}$ = ratio of kinematic viscosities of the liquid to vapor = ν_l/ν_v

ρ = mixture density = $\rho_l s + \rho_v(1-s)$

ρ_κ = "kinetic" mixture density = $\rho_l\lambda + \rho_v(1-\lambda)$

σ = interfacial tension

Ψ = streamfunction of the two-phase mixture, Eq. (15)

Subscripts

dry = dryout

l = liquid

r = relative

x = local

v = vapor

w = wall

1 Introduction

Buoyancy-driven two-phase flow in a porous medium is encountered in numerous important technological applications. Examples include boiling flow along an igneous intrusion in geothermal reservoirs and condensing flow adjacent to a cold surface in heat pipes and porous insulation materials. Recently, condensing flow has received particular attention, because the flow in the two-phase region, which results from the capillary force, is believed to exert a significant effect on film condensation heat transfer (Plumb, 1984; Shekarriz and Plumb, 1986; Majumdar and Tien, 1990; Plumb et al., 1990; Chung et al., 1992). An analogous effect can be expected for film boiling in porous media, although no study has been conducted.

Prior work (Plumb, 1984; Shekarriz and Plumb, 1986; Majumdar and Tien, 1990) has shown that the two-phase flow within the above context exhibits features similar to boundary-layer flow of single-phase fluids (Schlichting, 1968). Based on the separate flow model, these theoretical studies, however, neglect the vapor flow in order to render the problem analytically tractable. More specifically, the vapor phase is assumed to remain at a constant pressure; a two-phase flow problem is thus essentially reduced to the consideration of the liquid phase flow only. This approach, known as the unsaturated flow theory, is widely applied in hydrology (Morel-Seytoux, 1973), and the corresponding assumption is called the Richards approximation. While the theory has been shown to be a good approximation

[1] Department of Mechanical Engineering, The University of Iowa, Iowa City, IA 52242; present address: Assistant Professor, Department of Mechanical Engineering, University of Hawaii at Manoa, Honolulu, HI 96822.

[2] Associate Professor, Department of Mechanical Engineering, The University of Iowa, Iowa City, IA 52242; Mem. ASME.

Contributed by the Heat Transfer Division of THE AMERICAN SOCIETY OF MECHANICAL ENGINEERS. Manuscript received by the Heat Transfer Division September 1993; revision received January 1995. Keywords: Multiphase Flows, Phase-Change Phenomena, Porous Media. Associate Technical Editor: C. E. Hickox, Jr.

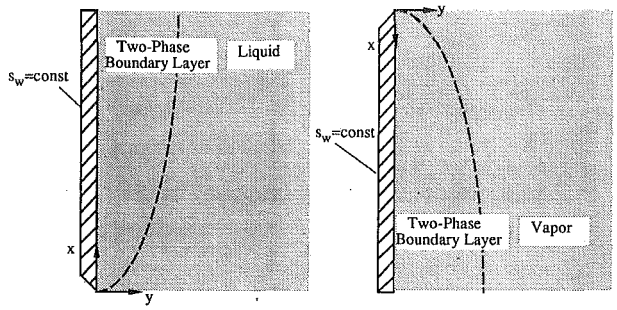

Fig. 1 Schematics of the physical problems and coordinate systems

in many hydrological situations, doubts remain regarding its validity in two-phase flow with phase change.

The goal of the present paper is twofold. First, based on a newly developed two-phase mixture model (Wang and Beckermann, 1993a), we perform a two-phase boundary layer analysis for buoyancy-driven two-phase (both condensing and boiling) flow in porous media, wherein only classical boundary layer approximations (Schlichting, 1968) are employed. A parallel theory for pressure-driven boiling flow has been presented by Wang and Beckermann (1993b). Second, using the present full two-phase solution, we quantitatively examine the validity of the unsaturated flow theory for buoyancy-driven condensing flow, so as to reveal the capillary effect on film condensation (or boiling) heat transfer in porous media more accurately.

2 Boundary Layer Analysis

Both boiling and condensing flows are dealt with in the present paper, as shown in Figs. 1(a) and 1(b). In each case, a two-phase zone where the liquid and vapor phases can coexist appears adjacent to the vertical wall. As the heat transfer at the wall is gradually enhanced, the liquid saturation at the wall approaches its respective limiting value, namely zero for boiling and unity for condensation. If the heat flux further exceeds this threshold point, a pure vapor or liquid film forms at the wall. A complete problem then involves multiple regions consisting of a single-phase film on the wall and the adjacent two-phase zone. The analysis in this paper focuses solely on the two-phase flow without a single-phase film covering the wall, followed by a brief discussion on its extension to a multiregion problem.

Like in all previous theoretical work, use is made of common assumptions, such as constant thermophysical properties, an isothermal two-phase zone, and the Darcian flow regime for both phases. However, simultaneous two-phase flow is considered in the following analysis, and hence the two-phase characteristics of the problem are fully retained.

2.1 Two-Phase Boundary Layer Equations. The present analysis is based on the two-phase mixture model recently proposed by the present authors (Wang and Beckermann, 1993a). The model is a mathematically equivalent but reformulated version of the classical separate flow model. The central idea underlying the approach is to view the two-phase system similar to a binary chemical mixture. Hence, a two-phase flow can uniquely be described by a mass-averaged mixture velocity, $\mathbf{u}$, and a diffusive flux, $\mathbf{j}$, which is defined as the difference between the mixture velocity and an individual phase velocity, $\mathbf{u}_l$ or $\mathbf{u}_v$. It has been shown in Wang and Beckermann (1993a) that the diffusive mass flux, $\mathbf{j}$, defined as

$$\mathbf{j} = \rho_l \mathbf{u}_l - \lambda \rho \mathbf{u} = -[\rho_v \mathbf{u}_v - (1 - \lambda)\rho \mathbf{u}] \tag{1}$$

is given by

$$\mathbf{j} = -D(s)\nabla s + f(s)\frac{K\Delta\rho}{\nu_v}\mathbf{g} \tag{2}$$

where $D(s)$ and $f(s)$ are the capillary diffusion coefficient and hindrance function, respectively, as defined in the Nomenclature. Throughout this paper, symbols without a subscript are reserved for mixture variables, while the subscripts v and l denote variables of the vapor and liquid phases, respectively. It can be seen from Eq. (2) that the diffusive mass flux is due to a combination of capillary diffusion and gravity-induced migration.

A set of boundary-layer equations has been derived by Wang and Beckermann (1993b) for the two-phase mixture motion. In the Cartesian coordinate systems shown in Fig. 1, the mixture mass conservation, mixture Darcy's law, and liquid mass conservation equations can be written as

$$\frac{\partial(\rho u)}{\partial x} + \frac{\partial(\rho v)}{\partial y} = 0 \tag{3}$$

$$\rho u = -\frac{K}{\nu}\left(\frac{\partial p}{\partial x} \pm \rho_\kappa g\right) \tag{4}$$

$$\rho \frac{d\lambda}{ds}\left(u\frac{\partial s}{\partial x} + v\frac{\partial s}{\partial y}\right) = \frac{\partial}{\partial y}\left(D\frac{\partial s}{\partial y}\right) \pm \frac{K\Delta\rho}{\nu_v} g \frac{df}{ds}\frac{\partial s}{\partial x} \tag{5}$$

where the mixture transport properties all depend on the local concentration (liquid saturation), s, and are defined in the nomenclature. The plus and minus signs in Eqs. (4) and (5) correspond to boiling and condensing flows, respectively. The pressure gradient in Eq. (4) is identical to the hydrostatic pressure gradient in purely buoyancy-driven flow. The reader is referred to Wang and Beckermann (1993a, b) for a detailed account of the two-phase mixture model as well as its boundary-layer simplified version. Here it is worth noting that Eqs. (3)–(5) strongly resemble the boundary-layer equations for single-phase binary mixture flow and transport in porous media.

The boundary conditions for Eqs. (3)–(5) are

$$\text{at } x = 0, \quad u = 0 \text{ and } s = \begin{cases} 1 & \text{boiling flow} \\ 0 & \text{condensing flow} \end{cases} \tag{6}$$

$$\text{at } y = 0, \quad v = 0 \text{ and } s = s_w \tag{7}$$

and

$$\text{when } y \to \infty \quad u = 0 \text{ and } s = \begin{cases} 1 & \text{boiling flow} \\ 0 & \text{condensing flow} \end{cases} \tag{8}$$

where s_w is the constant liquid saturation at the wall, with $s_w = 1$ representing the marginal condition for a pure liquid film to appear on the wall in the condensing case, and $s_w = 0$ corresponding to the dryout condition in the boiling case. The more general case of a saturation that varies along the wall has been examined by Chung et al. (1992). The present use of a uniform wall saturation enables a similarity solution to be obtained and a direct comparison with the results of Majumdar and Tien (1990) (see below).

Finally, the basic transport functions $k_{rl}(s)$, $k_{rv}(s)$, and $J(s)$ must be provided to determine the mixture mean transport properties (see Nomenclature). The following relative permeabilities and capillary pressure function are assumed in the present study:

$$k_{rl} = s^3 \; ; \; k_{rv} = (1 - s)^3 \tag{9}$$

and

$$J(s) = 1.417(1 - s) - 2.120(1 - s)^2 + 1.263(1 - s)^3 \tag{10}$$

where the irreducible liquid saturation has been taken to be zero for simplicity. This set of constitutive relations has been used in several previous studies (Shekarriz and Plumb, 1986; Ma-

jumdar and Tien, 1990; Wang and Beckermann, 1993b). Although more accurate relations may be found in the literature, the present choice allows for a direct comparison with the results of the previous studies.

2.2 Comparisons With Unsaturated Flow Theory. The unsaturated flow theory is valid in the limiting case where the vapor pressure can be assumed to be constant. Its parametric range can be revealed by a simple order-of-magnitude analysis. By application of the modified Darcy's law for two-phase flow, and taking the relative permeabilities to be of the order of unity, the ratio of the pressure drops across the two-phase zone can be approximated by

$$\frac{\Delta p_v}{\Delta p_l} \sim \frac{\mu_v v_v}{\mu_l v_l} = \frac{\nu_v}{\nu_l} \cdot \frac{\rho_l v_l}{\rho_v v_v} \tag{11}$$

Noting that the normal mixture velocity vanishes at the wall [Eq. (7)], the normal mass fluxes of the liquid and vapor phases can be assumed to be of the same order of magnitude (but opposite in sign). Then, Eq. (11) reduces to

$$\frac{\Delta p_v}{\Delta p_l} \sim \frac{\nu_v}{\nu_l} = 1/\bar{\nu} \tag{12}$$

where $\bar{\nu}$ is the ratio of the kinematic viscosities of the liquid to vapor. It can then be concluded that, for Δp_v to be negligibly small compared to Δp_l, as required in the unsaturated flow theory, $\bar{\nu}$ must approach infinity. In practice, however, $\bar{\nu}$ can be very small (e.g., $\bar{\nu} = 0.01466$ for a water–steam system at atmospheric pressure). This points out the possibility that the vapor phase may significantly retard the movement of the liquid phase, so that a full two-phase model must be adopted. Indeed, the most recent work by Chung et al. (1992) has realized this need and attempted to account for the vapor flow.

In the limiting case where $\bar{\nu} \to \infty$, it can be shown that

$$\frac{d\lambda}{ds} = O(\bar{\nu}^{-1}) \to 0; \quad D/D_c \to k_{rl}(s)[-J'(s)];$$

$$\frac{1}{\nu_v}\frac{df}{ds} \to \frac{1}{\nu_l}\frac{dk_{rl}}{ds} \tag{13}$$

Then, the governing equation for condensing flow, Eq. (5), reduces to

$$D_c \frac{\partial}{\partial y}\left\{k_{rl}(s)[-J'(s)]\frac{\partial s}{\partial y}\right\} - \frac{K\Delta\rho}{\nu_l} g \frac{dk_{rl}}{ds}\frac{\partial s}{\partial x} = 0 \tag{14}$$

This is exactly the key equation solved by Majumdar and Tien (1990) in their analysis using the unsaturated flow theory. Hence, the foregoing order-of-magnitude analysis is substantiated.

2.3 Similarity Solution. Equations (3)–(5) along with their boundary conditions admit a similarity solution by virtue of the following similarity variables:

$$\eta = \frac{y}{x}\mathrm{Ra}_x^{1/2}; \quad \Psi = D_c \mathrm{Ra}_x^{1/2} F(\eta) \quad \text{and} \quad s = s(\eta) \tag{15}$$

where the local two-phase Rayleigh number, Ra_x, is defined in the nomenclature, and Ψ is a streamfunction of the two-phase mixture such that $\rho u = \partial\Psi/\partial y$ and $\rho v = -\partial\Psi/\partial x$. This similarity transformation reduces Eqs. (3)–(5) to the following set of ordinary differential equations:

$$F' = \begin{cases} \bar{\nu} k_{rv} & \text{boiling flow} \\ k_{rl} & \text{condensing flow} \end{cases} \tag{16}$$

$$(\hat{D}s')' + \frac{1}{2}\frac{d\lambda}{ds} Fs' = \pm \frac{1}{2}\bar{\nu}\frac{df}{ds}\eta s' \tag{17}$$

The corresponding boundary conditions are

$$\text{at } \eta = 0, \quad F = 0 \quad \text{and} \quad s = s_w \tag{18}$$

$$\text{when } \eta \to \infty \quad F' = 0 \text{ and } s = \begin{cases} 1 & \text{boiling flow} \\ 0 & \text{condensing flow} \end{cases} \tag{19}$$

In the equations above the prime denotes the derivative with respect to η.

Equations (16) and (17) along with their boundary conditions (18) and (19) were numerically solved by the Gear stiff method (IMSL, 1991) combined with a shooting procedure for $s'(0)$. The singularity at $\eta = 0$, when the wall saturation approaches zero in the boiling case and unity in the condensing case, was treated in the same manner as in Wang and Beckermann (1993b). The present numerical procedures were validated by comparing the saturation profile obtained for the limiting case $\bar{\nu} \to \infty$ with that of Majumdar and Tien (1990), and excellent agreement was achieved.

The two-phase Sherwood number, defined again in the Nomenclature, stands for the dimensionless phase change rate at the wall. By the definition of the diffusive mass flux, Eq. (2), and using the similarity transformation, one can obtain

$$\mathrm{Sh}_x/\mathrm{Ra}_x^{1/2} = -\hat{D}(s_w)s'(0) \tag{20}$$

The Sherwood number is also a direct measure of the heat flux imposed at the wall, such that

$$\frac{q_w x}{h_{fg} D_c} = -\mathrm{Sh}_x = \hat{D}(s_w)s'(0)\mathrm{Ra}_x^{1/2} \tag{21}$$

where q_w denotes the wall heat flux. Integration of the equation above yields the average heat flux over the entire wall:

$$\frac{\bar{q}_w L}{h_{fg} D_c} = 2\hat{D}(s_w)s'(0)\mathrm{Ra}_L^{1/2} \tag{22}$$

which can be used to estimate the dryout heat flux in the boiling case when $s_w = 0$. In the condensing case, on the other hand, the liquid mass flux as calculated from the Sherwood number will reflect the capillary effect on film condensation heat transfer.

Having found the mixture velocity field from the similarity solution, the individual phase velocities can be calculated from Eq. (1) combined with Eq. (2). An important characteristic of the phase velocity fields can readily be inferred from the governing equations, Eqs. (16) and (17), by substituting the definition of the hindrance function given in the nomenclature. This leads to

$$[\hat{D}s' - \tfrac{1}{2}(\eta F' - F)\lambda]' = 0, \quad \text{boiling flow} \tag{23}$$

$$[\hat{D}s' + \tfrac{1}{2}(1-\lambda)(\eta F' - F)]' = 0, \quad \text{condensing flow} \tag{24}$$

Since the terms in parentheses actually represent the transverse components of the liquid and vapor velocities in boiling and condensing flows, respectively, one can conclude that the liquid (vapor) flow is exactly one-dimensional in the direction normal to the wall in boiling (condensing) flow. Physically, this is due to the fact that there is no driving force for liquid (vapor) motion in the longitudinal direction in the respective situation. For example, in boiling flow, the liquid momentum equation in the x direction reads

$$u_l = -\frac{Kk_{rl}}{\mu_l}\left(\frac{\partial p_l}{\partial x} - \rho_l g\right) \tag{25}$$

where the bracket on the right-hand side remains constant along the y direction, as implied by the boundary-layer approximations, and moreover is zero as $y \to \infty$. Hence, the axial liquid velocity, u_l, is zero everywhere.

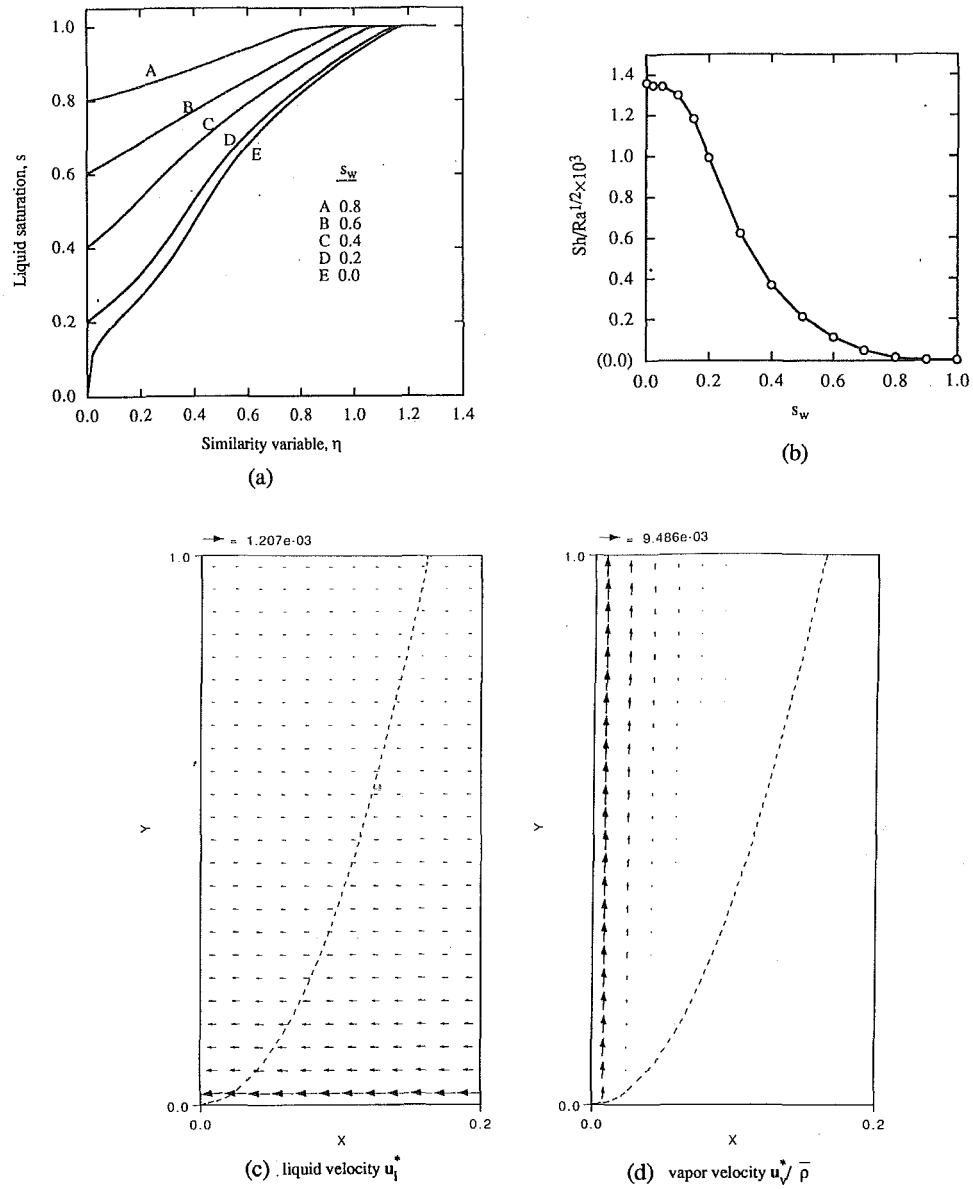

Fig. 2 Numerical results of two-phase boundary-layer boiling flow: (a) liquid saturation profiles for various wall saturations; (b) dimensionless phase change rate at the wall ($Sh_x/Ra_x^{1/2}$) as a function of wall saturations; (c) liquid flow field u_l^* for $s_w = 0$ and $Ra_L = 50$; and (d) corresponding vapor flow field $u_v^*/\bar{\rho}$. Here u is the normalized velocity, $u^* = u/(K\Delta\rho g/\mu_l)$, and the dashed line denotes the two-phase boundary layer edge.*

3 Results and Discussion

Numerical results are presented below separately for boiling and condensing flows. Inspection of the similarity equations reveals that the solution depends only on the viscosity ratio, $\bar{\nu}$, and the wall liquid saturation, s_w. Although the density difference between the two phases also has a substantial influence on the behavior of these types of flow, it does not enter the present similarity solution because of the definition of the mixture streamfunction, Ψ.

3.1 Boiling Flow. Illustrative calculations for boiling flow are performed for a water–steam system at atmospheric pressure. Hence, the value of $\bar{\nu}$ is fixed at 0.01466. Focus is placed on examining the effect of the wall liquid saturation (i.e., the wall heat flux) on two-phase flow behaviors as well as determining the dryout heat flux for boiling along a vertical plate in a porous medium.

Figure 2(*a*) shows the liquid saturation profiles with the wall saturation as the curve parameter. It can be noted that these profiles are complex in shape and possess several points of inflection, contrasting with the simple concentration profile in single-phase mass transfer problems. This feature results from the fact that the mean transport properties of a two-phase mixture are highly nonlinear and exhibit maxima at certain liquid saturations. The second distinctive feature of the saturation profiles shown in Fig. 2(*a*) is the sharp edges of two-phase boundary layers for all wall liquid saturations, since the capillary diffusion coefficient becomes extremely small.

The quantity $Sh_x/Ra_x^{1/2}$ is shown in Fig. 2(*b*) as a function of the wall liquid saturation. It is noted that it increases as the wall saturation decreases and finally converges to a value of 1.358×10^{-3} for the dryout condition ($s_w = 0$). Hence, the dryout heat flux is given by

$$\frac{\bar{q}_{dry}L}{h_{fg}D_c} = 2.716 \times 10^{-3}\,\mathrm{Ra}_L^{1/2} \tag{26}$$

or

$$\bar{q}_{dry} = 2.716 \times 10^{-3} \frac{h_{fg}\sigma}{\nu_l}\left(\frac{\epsilon K}{L^2}\right)^{1/4}\left[\frac{(\rho_l - \rho_v)gK}{\sigma}\right]^{1/2} \quad (27)$$

This result together with those obtained in a previous study on pressure-driven flow (Wang and Beckermann, 1993b) represent the useful bounds for boundary-layer boiling flows.

The axial mixture velocity, ρu (i.e., F'), can readily be evaluated from the saturation profiles via Eq. (16). Figures 2(*c*) and 2(*d*) instead depict the liquid and vapor phase velocity fields, respectively, in a typical two-phase boundary layer when $s_w = 0$ and $\mathrm{Ra}_L = 50$. The dashed line in these plots represents the edge of the boundary layer. The vapor moves primarily vertically due to the large density difference between liquid and vapor. The liquid is laterally entrained into the boundary layer, as indicated theoretically by Eq. (23). It is noteworthy that the entrainment is due to buoyancy-induced flow near the wall in the present problem, while the corresponding lateral motion in pressure-driven flow is caused by viscous displacement (Wang and Beckermann, 1993b).

3.2 Condensing Flow. The main objective of this subsection is to compare the present full two-phase solution with the approximate solution obtained by Majumdar and Tien (1990) using the unsaturated flow theory. The wall liquid saturation is chosen as unity (i.e., the marginal condition for a liquid film to appear). Hence, the viscosity ratio becomes the sole parameter. Figure 3(*a*) shows the liquid saturation profiles for different values of the viscosity ratio along with the curve obtained using the unsaturated flow theory (Majumdar and Tien, 1990). The latter is independent of the viscosity ratio $\bar{\nu}$. It can be seen that the curves indeed approach the limiting case represented by the unsaturated flow theory. However, the value of $\bar{\nu}$ for the unsaturated flow theory to hold is surprisingly large, i.e., $\bar{\nu} = 10^7$. Obviously, for all common fluids, this condition cannot be satisfied, indicating that the unsaturated flow theory is questionable when applied to the condensation problem under consideration. In fact, for a water–steam system at atmospheric pressure ($\bar{\nu} = 0.01466$), the saturation profile from the two-phase model greatly deviates from that predicted by the unsaturated flow theory.

As mentioned earlier, the capillary effect on condensation heat transfer is reflected by the liquid mass flux at the wall, j_w, or $\mathrm{Sh}_x/\mathrm{Ra}_x^{1/2}$ in a dimensionless form. Figure 3(*b*) depicts the influence of $\bar{\nu}$ on $\mathrm{Sh}_x/\mathrm{Ra}_x^{1/2}$. It is clearly seen that the unsaturated flow theory greatly overpredicts the dimensionless liquid mass flux, with $\mathrm{Sh}_x/\mathrm{Ra}_x^{1/2} = 0.288$, while the present two-phase model gives a value of only 4.35×10^{-3}. This 66-fold differ-

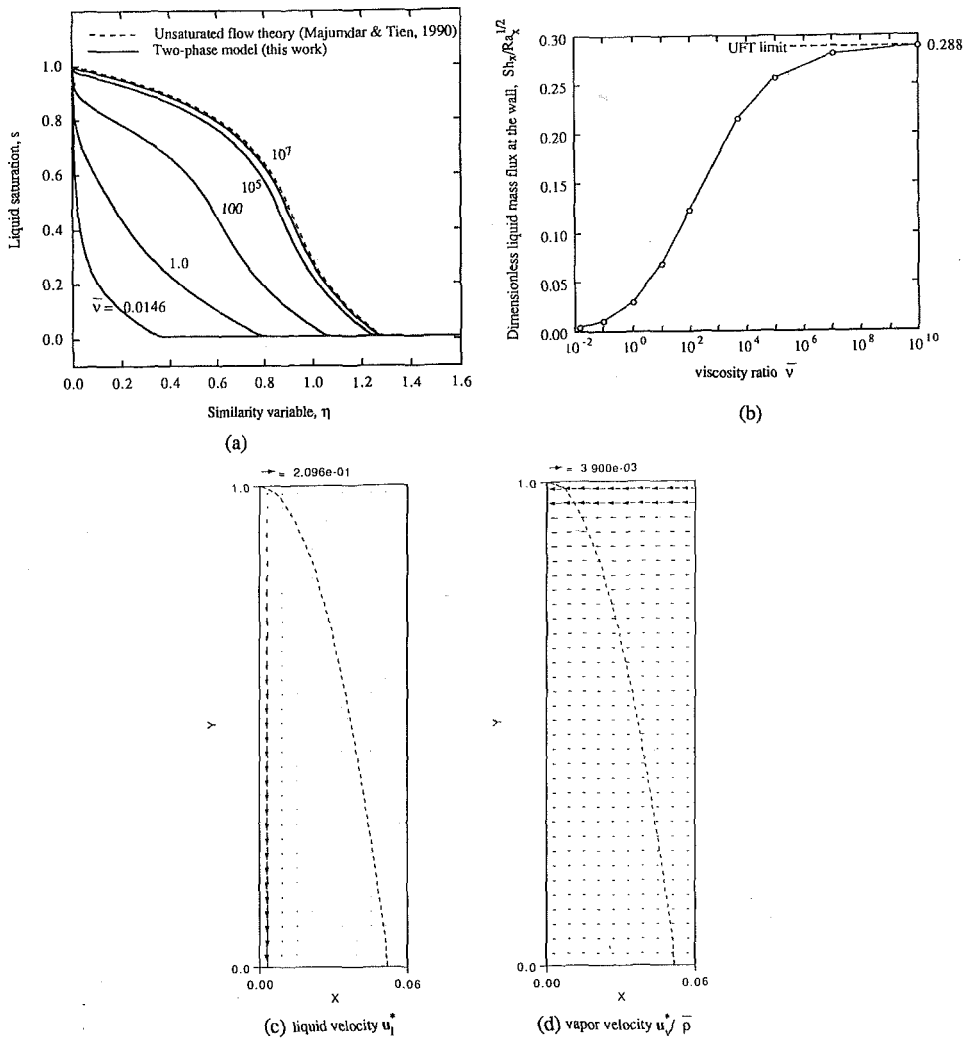

Fig. 3 Numerical results of two-phase boundary-layer condensing flow: (a) saturation profiles for various viscosity ratios ($\bar{\nu} = \nu_l/\nu_v$) and comparison with the unsaturated flow theory (Majumdar and Tien, 1990); (b) dimensionless liquid mass flux at the wall ($\mathrm{Sh}_x/\mathrm{Ra}_x^{1/2}$) as a function of the viscosity ratio; (c) liquid flow field u_l^* for $s_w = 1$, $\mathrm{Ra}_L = 50$, and $\bar{\nu} = 0.01466$; and (d) corresponding vapor flow field $u_v^*/\bar{\rho}$. Here u is the normalized velocity, $u^* = u/(K\Delta\rho g/\mu_l)$, and the dashed line denotes the two-phase boundary layer edge.*

ence suggests that the previous theoretical investigations based on the unsaturated flow theory (Plumb, 1984; Shekarriz and Plumb, 1986; Majumdar and Tien, 1990) have exaggerated the effect of the capillary force on condensation heat transfer in porous media. The overprediction results from the neglect of the vapor flow that is actually very strong due to the low vapor density.

Figures 3(c) and 3(d) displays the liquid and vapor flow fields in the two-phase boundary layer corresponding to a wall saturation of unity. The dashed line in these plots again denotes the edge of the boundary layer. Also note the large difference in the velocity scale given at the top of the figures. The liquid flow is essentially confined to a region very near to the wall where the vapor condenses into the liquid. As a result of its large density, the liquid moves primarily downward (however, the normal liquid velocity is not zero). The axial liquid velocity quickly diminishes with the normal distance, because it is proportional to the cubic of the liquid saturation, which furthermore has an extremely steep profile [see Fig. 3(a)]. Figure 3(d) shows that the vapor is only laterally entrained into the two-phase boundary layer, confirming the theoretical outcome of Eq. (24).

The present result agrees well with the assumption of Chung et al. (1992) regarding one-dimensional vapor flow. However, it should be kept in mind that the result is a consequence of the present analysis. Therefore, the theoretical framework itself is not subject to modifications in general situations where two-dimensional vapor flow is present, for example, in combined buoyancy- and pressure-driven two-phase flow.

Unfortunately, the available condensation experiments (White and Tien, 1987; Chung et al., 1992) appear to be inappropriate for validation of the present model. As pointed out by Kaviany (1991), the measured liquid film thicknesses in these experiments are of the same order as the bead diameters, causing a continuum treatment like the Darcy's formulation to break down. Furthermore, the experiments seem to be not representative of the capillary effect on condensation heat transfer. Indeed, as indicated by Plumb (1990), the physical models of Cheng (1981) and Chung et al. (1992) produce very similar results for the condensation rate under these experimental conditions, even though the latter is much more sophisticated and includes many non-Darcian effects as well as the capillary effect.

3.3 Combined Single- and Two-Phase Flow. Beyond the marginal condition where either $s_w = 0$ in boiling flow or $s_w = 1$ in condensing flow, a single-phase film appears on the wall in addition to the two-phase zone. In this case, the two-phase analysis needs to be extended to incorporate the single-phase flow within the film, and the latter can readily be dealt with, as done in many previous studies. The two-phase analysis is still valid except that the phase interface becomes permeable. As a result, the normal mixture velocity, v, is no longer zero as in Eq. (7), but must be obtained from the coupling between the single- and two-phase flows. Such an extension is not performed here for brevity.

4 Conclusions

Complementing a previous investigation on pressure-driven flow (Wang and Beckermann, 1993b), the present study analytically explores buoyancy-driven two-phase flow along a vertical plate in a capillary porous medium. Full two-phase similarity solutions were obtained for both boiling and condensing flows. Illustrative numerical results were presented for the liquid saturation profile, the flow fields of the two phases within the two-phase boundary layer, and the phase-change rate at the wall. The dryout heat flux in boiling flow was correlated with the fluid thermophysical properties and porous medium parameters. Experimental verification of these results is, however, necessary. For condensing flow, the present work improves previous approximate solutions based on the unsaturated flow theory, and further indicates that the theory is questionable for condensing flow. Accurate modeling of the capillary effect on film condensation heat transfer appears to require a full two-phase treatment. Further experimental work should also concentrate on this effect.

A comparison of the boiling and condensing boundary layer flows, as shown in Figs. 2(c, d) and 3(c, d), indicates that the boiling boundary layer is normally wider than the one in condensing flow, and that a two-phase crossflow pattern is representative of both boiling and condensing buoyancy-driven flows.

Acknowledgments

This work was supported by the National Science Foundation under Grant No. CTS-8957149 and by a University of Iowa Carver Scientific Research Initiative Grant.

References

Cheng, P., 1981, "Film Condensation Along an Inclined Surface in a Porous Medium," *Int. J. Heat Mass Transfer,* Vol. 25, pp. 983–990.

Chung, J. N., Plumb, O. A., and Lee, W. C., 1992, "Condensation in a Porous Medium Bounded by a Cold Vertical Surface," ASME JOURNAL OF HEAT TRANSFER, Vol. 114, pp. 1011–1018.

IMSL, 1991, *Manual of International Mathematical and Statistical Library,* Houston, TX.

Kaviany, M., 1991, *Principles of Heat Transfer in Porous Media,* Springer-Verlag, New York, pp. 569–572.

Majumdar, A., and Tien, C. L., 1990, "Effects of Surface Tension on Film Condensation in a Porous Medium," ASME JOURNAL OF HEAT TRANSFER, Vol. 112, pp. 751–757.

Morel-Seytoux, H. J., 1973, "Two-Phase Flows in Porous Media," *Adv. in Hydroscience,* Vol. 9, pp. 119–202.

Plumb, O. A., 1984, "Capillary Effects of Film Condensation in Porous Media," Paper No. AIAA-84-1789.

Plumb, O. A., 1990, "Heat Transfer During Unsaturated Flow in Porous Media," in: *Convective Heat and Mass Transfer in Porous Media,* NATO Advanced Study Institute, Aug. 6–17, Turkey.

Plumb, O. A., Burnett, D. B., and Shekarriz, A., 1990, "Film Condensation on a Vertical Flat Plate in a Packed Bed," ASME JOURNAL OF HEAT TRANSFER, Vol. 110, pp. 234–239.

Schlichtling, H., 1968, *Boundary Layer Theory,* 6th ed., McGraw-Hill, New York.

Shekarriz, A., and Plumb, O. A., 1986, "A Theoretical Study of Film Condensation Using Porous Fins," ASME Paper No. 86-HT-31.

Wang, C. Y., and Beckermann, C., 1993a, "A Two-Phase Mixture Model of Liquid-Gas Flow and Heat Transfer in Capillary Porous Media. Part I: Formulation," *Int. J. Heat Mass Transfer,* Vol. 36, pp. 2747–2758.

Wang, C. Y., and Beckermann, C., 1993b, "A Two-Phase Mixture Model of Liquid-Gas Flow and Heat Transfer in Capillary Porous Media. Part II: Application to Pressure-Driven Boiling Flow Adjacent to a Vertical Heated Plate," *Int. J. Heat Mass Transfer,* Vol. 36, pp. 2759–2768.

White, S. M., and Tien, C. L., 1987, "An Experimental Investigation of Film Condensation in Porous Structures," *Proc. 6th Int. Heat Pipe Conf.,* Grenoble, France.